TRANSFORM METHODS FOR PRECISION CONTINUUM AND CONTROL MODELS OF FLEXIBLE SPACE STRUCTURES

Victor D. Lupi, Research Assistant
Massachusetts Institute of Technology
Cambridge, Massachusetts

James D. Turner,* Controls and Dynamics Group Leader
Hon M. Chun,* Staff Scientist
Photon Research Associates, Inc.
Cambridge, Massachusetts

ABSTRACT

An open loop optimal control algorithm is developed for general flexible structures, based on Laplace transform methods. A distributed parameter model of the structure is first presented, followed by a derivation of the optimal control algorithm. The control inputs are expressed in terms of their Fourier series expansions, so that a numerical solution can be easily obtained. The algorithm deals directly with the transcendental transfer functions from control inputs to outputs of interest, and structural deformation penalties, as well as penalties on control effort, are included in the formulation. The algorithm is applied to several structures of increasing complexity to demonstrate its generality.

1. INTRODUCTION

The control of large flexible structures has become an important issue in recent years, primarily in the aerospace industry.[1] As larger structures continue to be deployed in space, the effects of control-structure interaction are becoming increasingly important. For example, stringent pointing requirements for space-based antennae make it necessary to isolate and suppress unwanted structural vibration caused by both slewing maneuvers and exogenous disturbances. Consequently, it becomes necessary to model structural flexibility when developing control laws for these types of structures.

Because disturbances and control forces generally act at discrete points on the structure, structural responses tend to exhibit wave propagation characteristics. Traditional finite element codes are unable to capture the high frequency behavior of such structures, due primarily to the spatial discretization associated with lumped parameter models. This limitation makes it particularly difficult to study the propagation of flexural waves within structures, since an extremely fine discretization is required to preserve the local wave-like characteristics of the disturbances. To overcome this problem, this paper develops a distributed parameter, system-based model, which deals directly with the governing partial differential equations that describe the structure.

Given the continuum model of a flexible structure, there remains the issue of identifying control methodologies that take advantage of the additional high frequency information available therein. Tzafestas[2] develops a distributed parameter analogue of the linear quadratic regulator theory. A distributed parameter Riccati equation, expressed in terms of spatial differential operators, is presented. Miller, Hall, and von Flotow[3] develop optimal control laws for power flow at structural junctions based on a travelling wave approach. The effect of the localized controller is to modify the wave scattering matrix at the junction in a way that minimizes the power flowing from the junction. MacMartin and Hall[4] consider optimal control of power flow in uncertain structures based on an H_∞ cost criterion. Closed-loop stability is guaranteed by minimizing the maximum power imparted to the structure over all frequencies. The optimal distributed control of a rigid spacecraft with flexible appendages is discussed by Breakwell.[5]

Skaar[6] presents closed-form open loop optimal control solutions for a simple structure. The cost function considered has the form:

$$J = \int_0^{t_f} \left\{ k_1 u(t)^2 + k_2 \dot{u}(t)^2 \right\} dt \qquad (1)$$

where u represents the control input, and k_1 and k_2 are constants. Terminal and integrated penalties on the structural deformations are not permitted. Rather, the terminal constraints are adjoined to the cost function with Lagrange multipliers. The exclusion of deformational penalties makes it possible to derive analytical solutions for certain types of maneuvers. Otherwise, the optimal control solution can, in general, only be obtained by numerical methods.

Analytical results are available for only the simplest of distributed parameter models, containing very few flexible elements. More often, a complex structure, such as a truss beam, is replaced by a single equivalent member in the continuum model. Such an approximation is usually accurate at low frequencies only. For general structures, the structural responses must be calculated numerically. The convolution integral representation technique developed by Skaar is generalized in this paper to handle arbitrary structural configurations.

A review of the continuum modeling approach is presented in section 2. The optimal control formulation is developed in section 3. Several examples of this method, applied to structures of increasing complexity, are then presented in section 4. Conclusions and recommendations can be found in section 5.

2. STRUCTURAL MODELING

2.1 Modeling of Flexible Elements

Traditional approaches for modeling complex structures have relied on finite element modeling techniques. This approach idealizes a structure as an assembly of many small pieces which are constrained to move together in a manner consistent with the internal elastic behavior of the underlying continuum model. These techniques are powerful and widely used. However, they suffer from various modeling idealizations which limit the accuracy of behavior predictions, particularly for high frequency.

In order to better model the high frequency behavior of

*Member, AIAA

elastic frame-like structures, a continuum approach is presented in this paper which overcomes the conventional limitations of traditional finite element modeling techniques. The continuum method (also known as the exact finite element, distributed parameter, or dynamic stiffness method), deals directly with the governing partial differential equations for the individual elastic elements to eliminate the explicit time dependence in the equations of motion. The Laplace transform is employed to convert the governing partial differential equations into ordinary differential equations in the spatial dimension. For common element models (e.g., rods in torsion, Bernoulli-Euler beams in bending), simple analytical solutions to these equations exist. The resulting solutions are explicit functions of the generally complex frequency parameter, s, which has been introduced through the application of the Laplace transform technique.

As an example, consider the case of a rod in torsion, shown in Fig. 1. The governing partial differential equation is

$$GJ\theta''(x,t) + mr^2\ddot{\theta}(x,t) = \tau(x,t) \tag{2}$$

where θ is the cross sectional angle of twist, GJ is the torsional rigidity, m is the mass per unit length, r is the cross sectional radius of gyration, $(\,)'=\partial(\,)/\partial x$, $\dot{(\,)}=\partial(\,)/\partial t$, and τ is the distributed torque. Applying the Laplace transform, we obtain

$$\theta''(x,s) + \frac{mr^2s^2}{GJ}\theta(x,s) = 0 \tag{3}$$

where initial conditions and distributed forcing along the element have been temporarily neglected. The general solution follows as:

$$\theta(x,s) = A(s)\cos\beta x + B(s)\sin\beta x, \quad \beta^2 = -\frac{mr^2}{GJ}s^2 \tag{4}$$

where the functions A(s) and B(s) depend on the constraints imposed at the boundaries of the element. To simplify the mathematical developments, a structural state vector is defined for the elastic element as follows:

$$y(x,s) = \begin{bmatrix} \theta(x,s) \\ T(x,s) \end{bmatrix} \tag{5}$$

where T represents the net torque resultant along the rod. With knowledge of the state at one boundary of the element, it is then possible to determine the state at any internal location. A frequency-dependant spatial transition matrix is used to propagate the system state to arbitrary element locations. Its transcendental elements can be thought of as spatially varying transfer functions. For this example, the transition matrix can be shown to be

$$\Phi(x,s) = \begin{bmatrix} \cos\beta x & \frac{1}{GJ\beta}\sin\beta x \\ -GJ\beta\sin\beta x & \cos\beta x \end{bmatrix} \tag{6}$$

and

$$y(x,s) = \Phi(x,s)\, y(0,s) \tag{7}$$

Alternatively, when the displacements at the boundaries are known, they can be related to the forces. This is accomplished by a dynamic stiffness matrix. Its name derives from the stiffness matrix associated with the traditional finite element method. For the rod in torsion, this matrix is given by

$$K(s) = \frac{GJ\beta}{\sin\beta l}\begin{bmatrix} \cos\beta l & -1 \\ -1 & \cos\beta l \end{bmatrix} \tag{8}$$

where l is the length of the rod.

In addition to torsional rods, the formulation also handles Euler beams in bending in two directions and axial rods. Timoshenko beams can also be included as continuum elements.

Because the continuum method treats each elastic member as a single element, no spatial discretization is required. This is in marked contrast with traditional finite element methods, where each element must be lumped into several segments. As a result, the continuum model is valid at all frequencies, insofar as the partial differential equation represents the actual physical structure. In contrast, the spatial discretization associated with the finite element approach creates a computational burden for even the simplest of structures (each flexible element is typically broken down into more than ten segments). This significant reduction in the number of discrete modeling elements required makes the continuum method more attractive from a computational point of view.

Another advantage to the frequency domain modeling approach is the ease with which damping is incorporated into the structural model. For internal damping (where energy is dissipated as heat within the structural elements) the static bending, axial or torsional stiffness is replaced by a complex valued function of the complex frequency. The functional relationship depends on the type of damping modeled. For example, a fractional derivative damping model scales the static stiffness by the square root of the complex frequency.[7] This type of damping model is extremely difficult to implement in time domain formulations, and requires a knowledge of the entire past history of the deformation of the structural element. For external damping (where structural energy is dissipated to the surroundings) the mass per unit length is replaced by a frequency-dependant parameter.[7]

2.2 Assembly of Elements

The assembly of flexible elements into a complex frame-like structure is accomplished using the method of local/global coordinates,[7] which is implemented in most finite element software. The structure to be modeled is divided into a set of flexible elements and a set of rigid joints, which attach to any number of flexible elements at their respective boundaries, as shown in Fig. 2. External forces are applied at the joints only, but the deformation of the structure is available at all points. (The case of a concentrated force applied within a

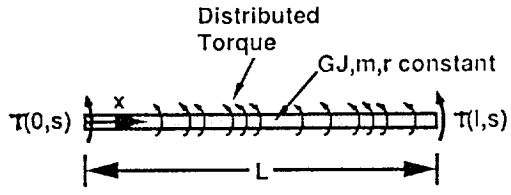

Fig. 1: Example of a distributed parameter element: a rod in torsion.

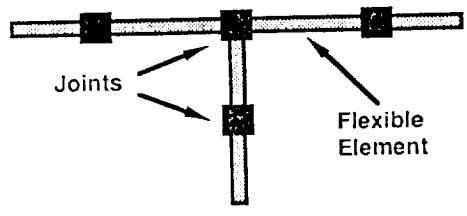

Fig. 2: Generic frame-like structure.

flexible element is treated by breaking the member into two continuous elements connected by a massless joint. Modeling distributed forcing is somewhat more difficult.) Massive joints are modeled by dynamic stiffness matrices as well, so that their contribution to the structural response at all frequencies is retained.

The topology of the structure is given by a connectivity matrix, which relates the local displacements of the structural elements (both flexible and rigid) to a set of global displacements which uniquely describe the location and orientation of all joints in the structure. The applied forces at the joints are defined in a dual manner, so that for every global displacement there exists a global forcing input at the same point and in the same direction. It is then a simple matter to compute the dynamic stiffness matrix for the structure as a whole at any given complex frequency. The individual stiffness matrices are first arranged in a large block diagonal matrix. This matrix is then post- and pre-multiplied by the connectivity matrix and its transpose, respectively, resulting in the system dynamic stiffness matrix.

Because the dynamic stiffness matrix is transcendental in nature, computing natural frequencies is not a simple matter of solving an eigenvalue problem, as is the case for the finite element approach. Rather, the stiffness matrix must be computed at many frequencies in order to gradually converge on each modal frequency. However, a powerful algorithm is available which rapidly converges on these eigenfrequencies.[8] The algorithm works for undamped systems only, and additional root-searching algorithms must be employed when structural damping is modeled.[7]

The system dynamic stiffness matrix can be inverted, if desired, yielding the dynamic flexibility matrix for the structure. Its elements can be thought of as transfer functions from the joint forces to the joint displacements or as admittance functions. This flexibility matrix, in conjunction with the flexible element spatial transition matrices, enables the straightforward calculation of the transfer function from any joint force to any point on the structure.

2.3 Inverse Laplace Transform

In the frequency domain, the responses at various locations within a linear elastic structure to multiple control inputs are determined by exploiting the principle of superposition. The set of responses, $y_i(s)$, are expressed as

$$y_i(s) = \sum_{j=1}^{m} g_{ij}(s)\, u_j(s), \quad i = 1,\ldots,r \tag{9}$$

where $g_{ij}(s)$ is the transfer function from the j'th input, $u_j(s)$, to the i'th output, $y_i(s)$. These equations can be expressed in more compact form using matrix notation:

$$\mathbf{y}(s) = \mathbf{G}(s)\mathbf{u}(s) \tag{10}$$

The matrix $\mathbf{G}(s)$ is the dynamic flexibility matrix for the given structure, or some partition of it, depending on the inputs and outputs considered.

The time response vector corresponding to $\mathbf{y}(s)$ is available via the inverse Laplace transform, given by

$$\mathbf{y}(t) = \frac{1}{2\pi j} \int_{\alpha-j\infty}^{\alpha+j\infty} \mathbf{y}(s)\, e^{st}\, ds \tag{11}$$

where the integration path is known as the Bromwich contour.[9] For finite dimensional systems, a residual expansion is used in lieu of Eq. (11) to compute the time responses analytically. The same can be done for distributed parameter systems, except that the expansion has an infinite number of terms and must therefore be truncated at some point. However, greater numerical accuracy is possible by working with Eq. (11) directly. The frequency domain response is tabulated for values of complex frequency equally spaced along the Bromwich contour, and a numerical procedure converts this data into a response history evaluated at equal spaces in time.[10]

Because this approach utilizes frequency domain representations of the control inputs, it circumvents the computationally expensive calculation of convolution integrals. Furthermore, signals that cannot be represented by finite dimensional state space models are easily handled in the frequency domain. For example, the implementation of a time delay simply requires multiplication of the frequency domain data by a suitable exponential of the complex frequency before the inverse Laplace transform algorithm is invoked. Implementing such a time delay on a modal basis requires a truncated series expansion of the complex exponential (such as a Padè approximation), with many terms needed to obtain an accurate representation.

3. OPTIMAL CONTROL FORMULATION

With the continuum modeling approach described above, it is possible to recast a class of optimal control problems into a convenient form, from which optimal control trajectories are easily calculated. This form is applicable to a completely general frame-like structure (although applying this method to structures containing plates and membranes is the subject of current research[11]), with multiple control inputs and multiple outputs. The class of problems discussed here are fixed-time, linear quadratic, open loop control problems with penalties on control effort, position and velocity of various output points on the structure, and structural deformation. Thus, the cost functional has the form

$$J = [\mathbf{y}(t_f) - \mathbf{y}_d]^T \mathbf{H} [\mathbf{y}(t_f) - \mathbf{y}_d] + \int_0^{t_f} \left\{ [\mathbf{y}(t_f) - \mathbf{y}_d]^T \mathbf{Q} [\mathbf{y}(t_f) - \mathbf{y}_d] + \mathbf{u}(t)^T \mathbf{R}\, \mathbf{u}(t) \right\} dt \tag{12}$$

where $\mathbf{H}$, $\mathbf{Q}$ and $\mathbf{R}$ are weighting matrices, and $\mathbf{y}_d$ is the vector of desired output values. It should be noted that $\mathbf{y}_d$ represents the physical output variables of interest, and is not related to the outputs of some state variable representation of the system.

Traditionally, the dynamics of the system are adjoined to this functional via a costate vector as differential equation constraints. However, because the structural transfer functions are transcendental and infinite dimensional, a finite dimensional costate vector cannot be defined. Tzafestas[2] succeeded in identifying a distributed parameter optimal control solution which incorporates an infinite dimensional costate. This solution represents the distributed parameter analogue of the Riccati differential equation for finite dimensional systems. However, the method is not immediately applicable to complex structures, where more than one partial differential equation is involved. Even the case of a single beam in bending presents considerable difficulty.[12]

One alternative to adjoining an infinite dimensional costate is modal truncation. The high frequency modes of the structure are simply ignored, and the dynamics of the structure is approximated with a finite dimensional state space realization. However, in order to take advantage of the "exactness" of the continuum modeling approach, it seems appropriate to avoid modal truncation altogether. Instead, we express each response as the convolution of impulse responses with control inputs. This yields for the cost function

$$J = \left[\int_0^{t_f} G(t_f-\tau)u(\tau)\,d\tau - y_d\right]^T H \left[\int_0^{t_f} G(t_f-\tau)u(\tau)\,d\tau - y_d\right] + \int_0^{t_f} \left\{ \left[\int_0^{t} G(t-\tau)u(\tau)\,d\tau - y_d\right]^T Q \left[\int_0^{t} G(t-\tau)u(\tau)\,d\tau - y_d\right] + u(t)^T R u(t) \right\} dt \quad (13)$$

where G(t) is the matrix of impulse responses from each control input to each output, as defined in section 2.3. These convolution integrals need not be computed directly, as they are the inverse transforms of the appropriate transfer functions multiplied by the associated control inputs. Taking variations in **u**, we are left with an integral equation which, except for a very small number of special cases, is difficult or impossible to solve in closed form. It is therefore necessary to express the control inputs as weighted sums of an appropriate set of basis functions which span the function space of allowable control inputs. For fixed time problems, the Fourier series is a good candidate, leading to

$$u(t) = \begin{bmatrix} f(t)^T c_1 \\ f(t)^T c_2 \\ \vdots \\ f(t)^T c_m \end{bmatrix} = F(t)^T c, \quad f(t) = \begin{bmatrix} 1 \\ \sin \pi t/t_f \\ \cos \pi t/t_f \\ \vdots \\ \sin n\pi t/t_f \\ \cos n\pi t/t_f \end{bmatrix} \quad (14)$$

where

$$F(t) = \begin{bmatrix} f(t) & & & \\ & f(t) & & \\ & & \ddots & \\ & & & f(t) \end{bmatrix}, \quad c = \begin{bmatrix} c_1 \\ c_2 \\ \vdots \\ c_m \end{bmatrix} \quad (15)$$

The cost functional now depends only upon a constant vector, **c**, representing the coefficients in the Fourier series expansions of the control inputs. The resulting cost functional is quadratic in the coefficient vector, and the minimization problem is straightforward, yielding:

$$c = A^{-1} B y_d \quad (16)$$

where

$$A = Y(t_f)^T H Y(t_f) + \int_0^{t_f} \left\{ Y(t)^T Q Y(t) + F(t)^T R F(t) \right\} dt \quad (17)$$

$$B = Y(t_f)^T H + \int_0^{t_f} \left\{ Y(t)^T Q \right\} dt \quad (18)$$

and

$$Y(t) = \int_0^{t} G(t-\tau) F(\tau)\,d\tau \quad (19)$$

Once again, the convolution of impulse responses with basis function inputs can be calculated via the inverse Laplace transform:

$$Y(t) = L^{-1}\{G(s)F(s)\} \quad (20)$$

Furthermore, these basis responses can be computed *a priori*, provided that the forcing locations and structural deformation penalty locations are known in advance. This makes it possible to try a large number of cost functionals without repeatedly calculating the responses to basis inputs. It should be mentioned that a large amount of memory is required to store this data.

A unique advantage of this approach is that it readily accommodates penalties in higher derivatives of both control effort and physical deformation. In the frequency domain, differentiation merely requires multiplication of the data by the Laplace transform variable. The inverse transformation will then produce the derivative of the original signal. Higher order derivatives are obtained by multiplying by higher powers of the complex frequency. Incorporating higher derivative penalties in the traditional optimal control formulation is considerably more difficult.

Special constraints on the control histories are treated by adjoining the constraints via Lagrange multipliers. An example is the requirement that the controls be continuous at the beginning and end of the maneuver. This implies that the controls go to zero at the initial and final times. Two Lagrange multipliers are therefore introduced for each control input. Performing the minimization, we obtain

$$\begin{bmatrix} c \\ \lambda_1 \\ \lambda_2 \end{bmatrix} = \begin{bmatrix} A & F(0) & F(t_f) \\ F(0)^T & 0 & 0 \\ F(t_f)^T & 0 & 0 \end{bmatrix}^{-1} \begin{bmatrix} B y_d \\ 0 \\ 0 \end{bmatrix} \quad (21)$$

where λ_1 and λ_2 are Lagrange multiplier vectors corresponding to the control constraints at the initial and final times, respectively.

It should be noted that the only approximation in the entire development involves expressing the control inputs in terms of the basis functions. The dynamics of the entire structure is accounted for, since the impulse responses are exact (insofar as the original equations represent physical reality). Also, the structural deformations are assumed to be small, so that linearization does not introduce significant errors. As a result, large angle slew maneuvers are not included in this class of problems. It is possible, however, to express structural deformations with respect to a nominal condition during a large angle slew, and then linearize about that reference.

It is important to note the difference between the approximations made in the continuum approach and those made in control systems based on finite element models. Typically, a finite element model is used to determine a truncated state space realization of the system. The control system is then designed using standard methodologies, such as linear quadratic regulator (LQR) or H_∞ theory. The modeling error associated with modal truncation must then be considered in assessing the performance of the system. In contrast to this, the continuum approach retains all modes of the system and therefore has no modeling error associated with it, provided that the original partial differential equations represent the physical system exactly. The only limitation to this approach is therefore the number of basis functions chosen to represent the control signals. Using the Fourier series expansion essentially places a limit on the bandwidth of the control inputs. If the bandwidth of the physical controls are known in advance, the number of basis functions used in the calculations can be adjusted accordingly. The resulting control history would then indeed be optimal for that set of physical controls.

4. EXAMPLES

4.1 Rigid Mass with Flexible Appendage

In an earlier analytical study by Skaar[6], the open loop control of a rigid mass with a flexible appendage, shown in Fig. 3, was studied. In his work, deformational penalties were not incorporated into the cost function; rather, the terminal conditions were adjoined to the cost functional as constraints. Skaar derived analytical expressions for impulse responses of the simple mass/appendage structure and thus obtained closed form optimal control solutions for the structure. His approach does not readily generalize for more complex structures. In contrast, the formulation presented here readily generalizes for realistic complex structures. Nevertheless, the mass/appendage structure is used as a first example to validate the optimal control formulation.

The maneuver involves translating the mass a distance of 10 meters along the axis of the flexible appendage, bringing it to rest with minimal residual energy and post-maneuver drift after 20 seconds. The first case places terminal penalties on the final position and velocity of the rigid mass and on a point 4/5 of the length along the flexible appendage. A small penalty is also placed on control rate, and 17 basis functions are used to approximate the control input. The results, shown in Fig. 4, indicate that the terminal conditions are matched, and residual energy is minimized. The second case places additional terminal penalties on points along the flexible appendage, as well as en-route (integrated) penalties on structural deformation at these points. As shown in Fig. 5, the magnitude of the structural deformation during the maneuver is reduced slightly (about 15%), and large deformation occurs over smaller intervals of time, resulting in a lower RMS displacement of the tip of the appendage over the maneuver interval. The terminal conditions are again matched. In the final case, the member stiffness is reduced by a factor of four, so that the primary modal frequency of the structure corresponds approximately

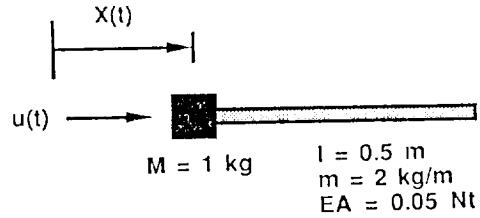

Fig. 3: Mass/flexible appendage system.

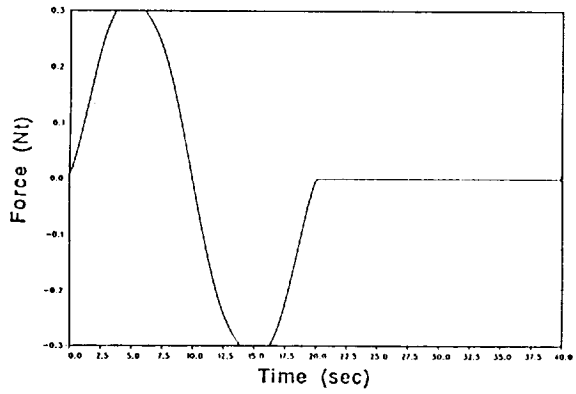

(a)

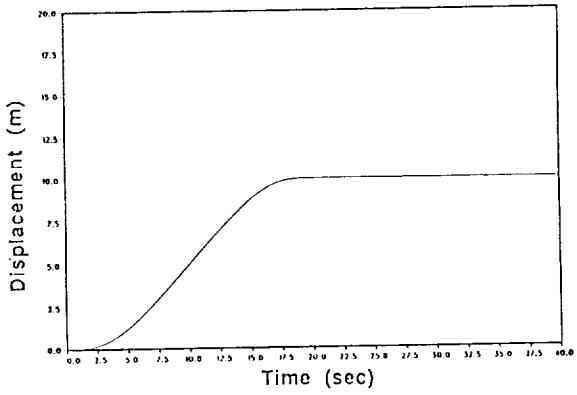

(b)

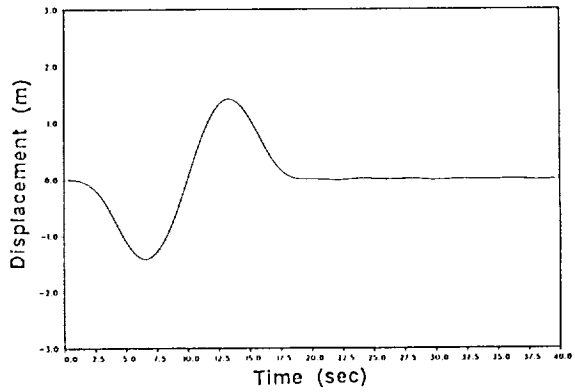

(c)

Fig. 4: Results of optimal maneuver of mass/flexible appendage system (case #1): (a) control force applied to rigid mass, (b) position of rigid mass, (c) deformation of tip of flexible appendage with respect to position of rigid mass.

with the frequency of the first basis function of the control input. The results of this case, presented in Fig. 6, indicate that the control input has been adjusted so that excitation of the primary mode of the structure is suppressed, at the expense of increased control effort. Again, the terminal conditions are matched, and residual internal energy is minimal.

4.2 Starfish Configuration

A typical model for a spacecraft with flexible appendages is the starfish configuration, shown in Fig. 7. It consists of a rigid hub, to which four flexible arms are attached. At the end of each arm is a rigid mass. Control inputs are available at the hub and at the tips of two of the flexible arms.

For this structural model, two maneuvers are presented. The first is an in-plane translation of 0.1 meter in the direction of one of the flexible appendages, with a final time of 5 seconds and all three control inputs available. Terminal penalties are placed on the position and velocity of the hub, as well as at three locations along the two arms whose axes lie in a direction perpendicular to the motion. It is anticipated that the control forces will excite bending vibration in these perpendicular members due to their inertia. Identical magnitude

and velocity penalties are also placed on the three control inputs. The results of this maneuver are shown in Fig. 8. The forces provided by the thrusters at the two appendages are identical (except for their sign) and differ slightly from the control history of the thruster at the hub. This discrepancy compensates for the inertia of the flexible arms, bringing the system to the final desired state with minimal residual energy.

The second maneuver involves a small (0.1 radian) counter-clockwise in-plane rotation about the hub in addition to the translation of the previous maneuver, in order to demonstrate the ability of the optimal control approach to handle multiple final conditions. Here, only the lateral forces at the tips of two of the appendages are available. Also, terminal position and velocity penalties are placed on two points along all four arms, as well as on the central hub, and the final time remains unchanged. The results are presented in Fig. 9. Again, the incorporation of state penalties involving structural deformation succeeds in minimizing residual internal energy at the terminal time. As previously mentioned, the linear control solution applied to this type of maneuver is only appropriate for small rotations and angular rates. For large rotations, nonlinear kinematics must be considered, whereas for large angular rates, gyroscopic forces become significant.

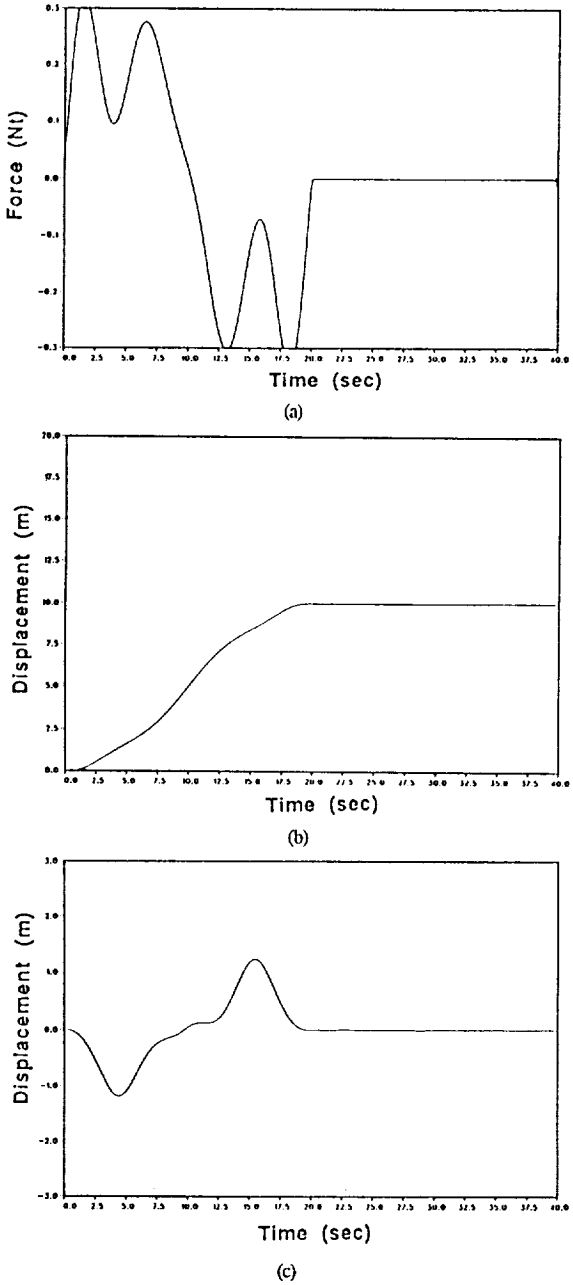

Fig. 5: Results of optimal maneuver of mass/flexible appendage system (case #2): (a) control force applied to rigid mass, (b) position of rigid mass, (c) deformation of tip of flexible appendage with respect to position of rigid mass.

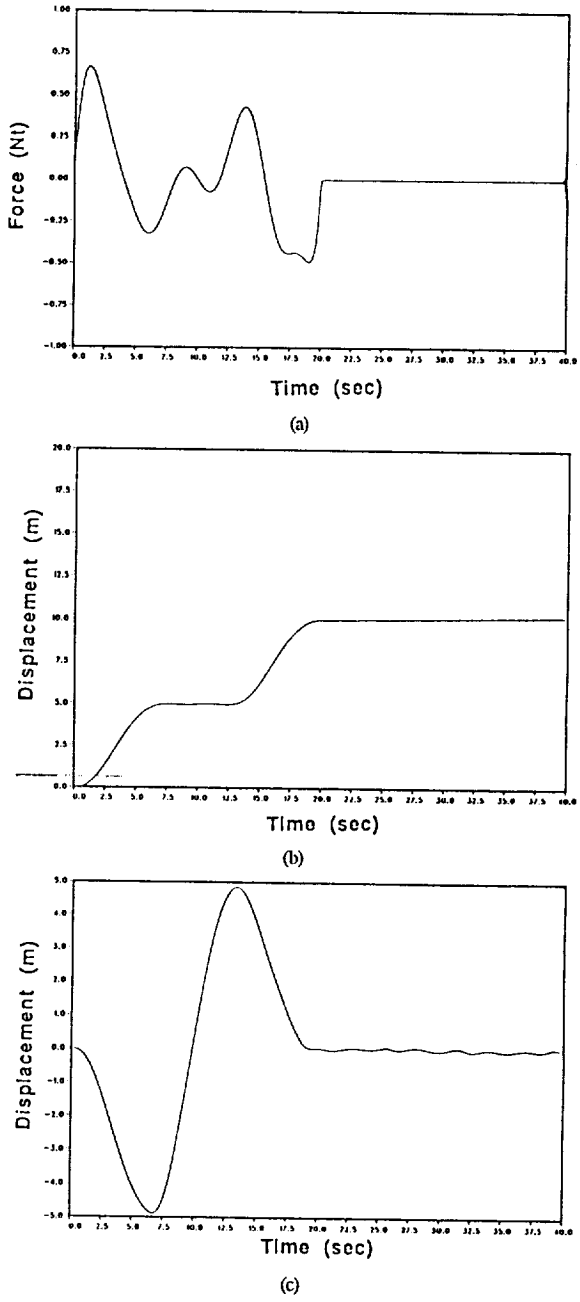

Fig. 6: Results of optimal maneuver of mass/flexible appendage system with reduced axial stiffness (case #3): (a) control force applied to rigid mass, (b) position of rigid mass, (c) deformation of tip of flexible appendage with respect to position of rigid mass.

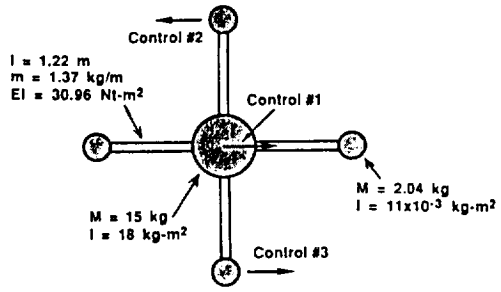

Fig. 7: Diagram of starfish configuration.

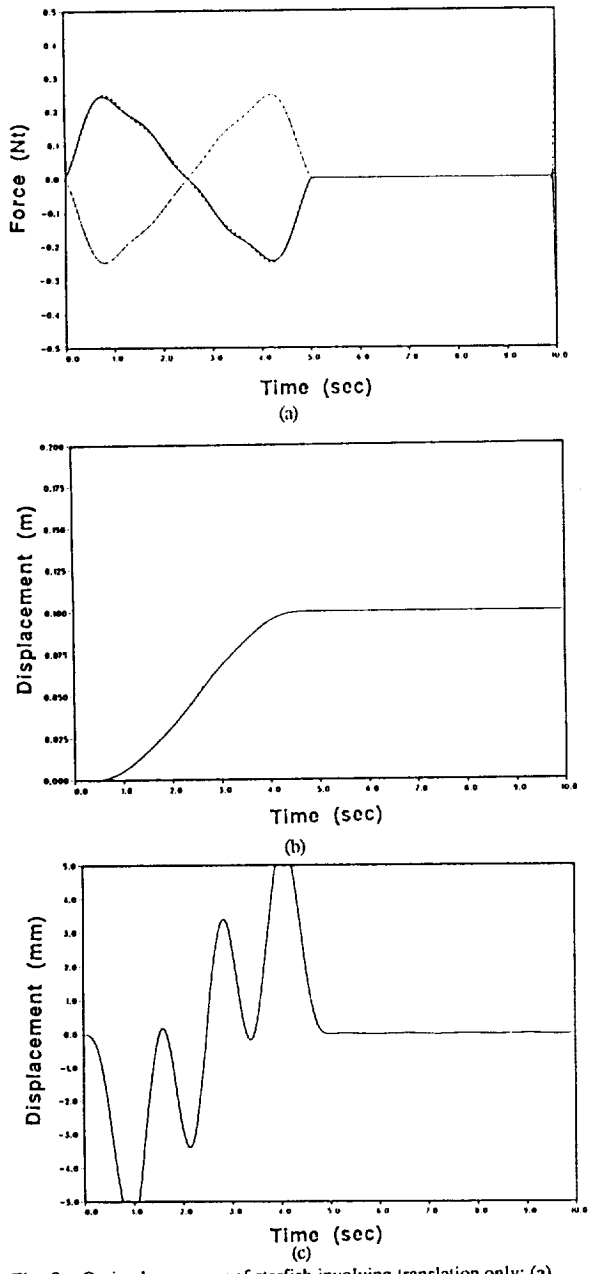

Fig. 8: Optimal maneuver of starfish involving translation only: (a) control forces applied at hub (solid line), thruster #2 (dotted line), and thruster #3 (double dotted line), (b) position of hub, (c) relative transverse deflection of flexible arm associated with control #2.

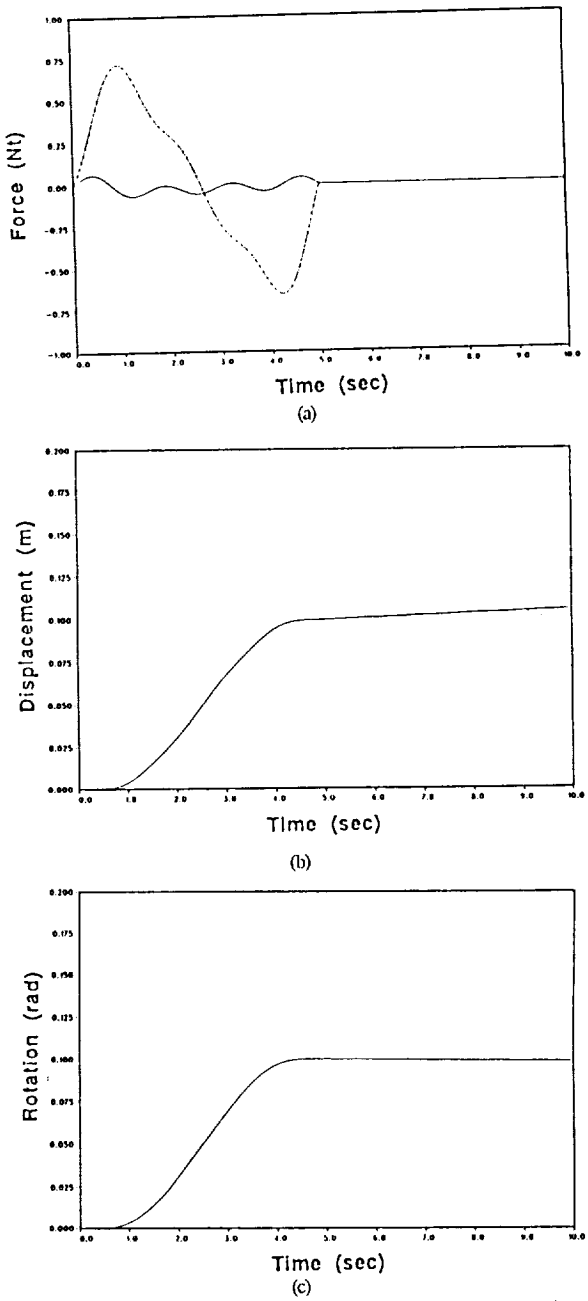

Fig. 9: Optimal maneuver of starfish involving translation and rotation: (a) Control forces applied to thruster #2 (solid line) and thruster #3 (dotted line), (b) translation of central hub, (c) rotation of central hub.

4.3 SCOLE Structure

The final example is a complex three dimensional structure proposed by NASA as a design challenge.[13] The Spacecraft COntrol Laboratory Experiment, shown in Fig. 10, consists of a rigid shuttle and hexagonal truss antenna connected by a flexible mast. Previous authors have treated the antenna as being rigid. In this paper, however, the flexibility of the antenna is considered. Figure 11 shows the transfer functions from a torque applied to the shuttle along about the axis of the mast to various points along the mast and antenna for both the rigid and flexible antenna models. A validation of this structural model with a traditional finite element code is

currently underway. As indicated in the figure, the flexibility of the antenna has a considerable effect on the transfer functions at higher frequencies. It is therefore appropriate to include a dynamic model for the antenna when applying the optimal control algorithm.

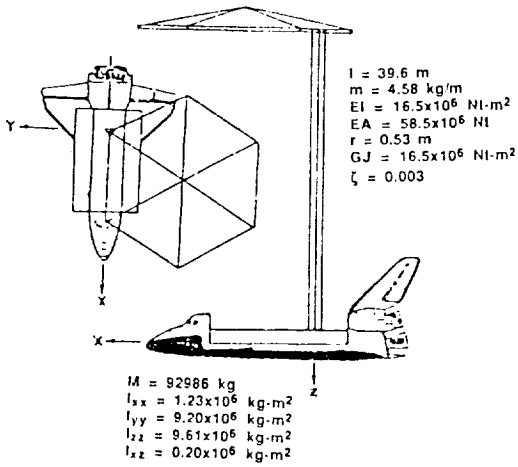

(a)

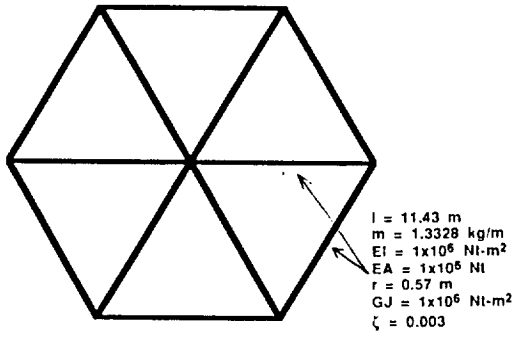

(b)

Fig. 10: The SCOLE experiment: (a) Shuttle and flexible mast properties, (b) flexible antenna model used in this study.

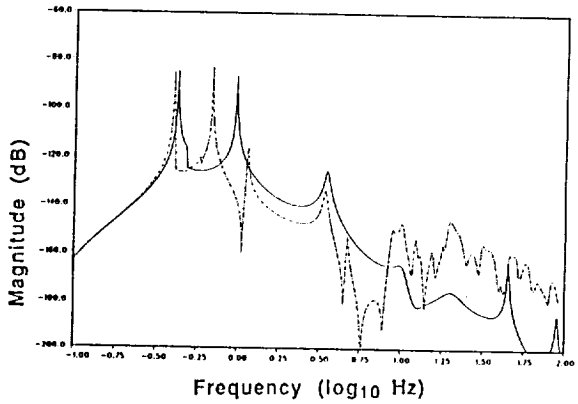

(a)

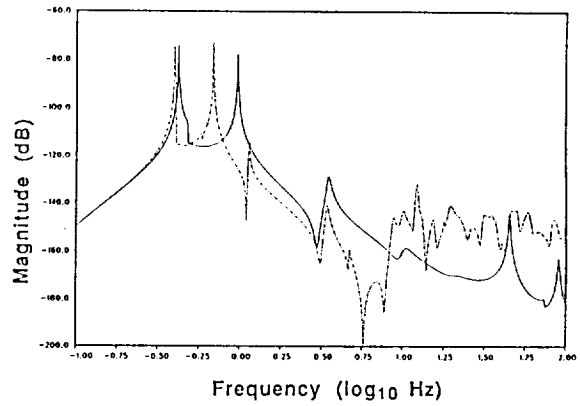

(b)

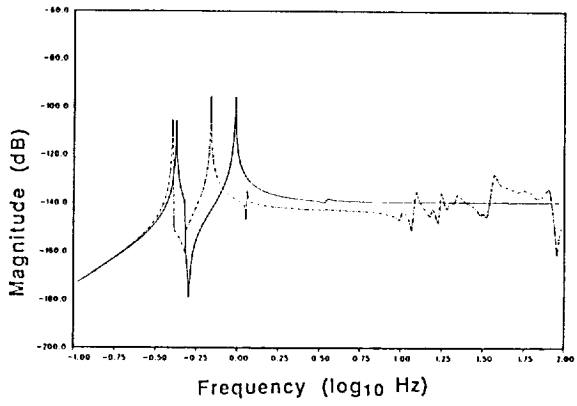

(c)

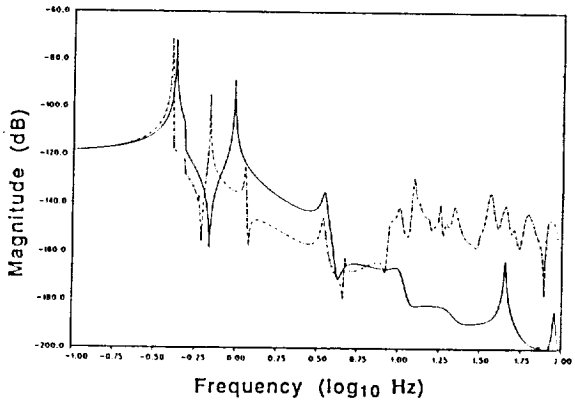

(d)

Fig. 11: Some transfer functions from control torque applied to shuttle along mast axis to inertial accelerations at various points on SCOLE structure for a rigid antenna (solid lines) and for a flexible antenna (dotted lines): (a) torsion of midpoint of mast, (b) torsion of mast at antenna junction, (c) transverse deflection of mast in pitching direction at antenna junction, (d) deflection, in plane of antenna, of antenna hub.

The SCOLE maneuver presented here consists of a 0.1 radian rotation about the z-axis of the shuttle. The three dimensional model used in the optimal control formulation incorporates 52 partial differential equations, which account for axial, torsional, and bending vibration in the mast and each of the twelve antenna elements. The shuttle is modeled as a massive rigid body with six degrees of freedom. Torque

controls directed along the z-axis are placed at either end of the mast. Due to the asymmetry of the structure, bending/torsion coupling is expected. Consequently, roll and pitch torque controls are also located on the shuttle. In the cost functional, equal magnitude and rate penalties are placed on all four controls. Large terminal penalties are applied to the roll, pitch and yaw angles of the shuttle, as well as the torsional deformation of the mast at its midpoint and at the mast/antenna junction. The maneuver time is ten seconds.

The results of the SCOLE slew are shown in Fig. 12. Because of the conventions used in defining the axes at the nodal points, the torques applied to the ends of the mast are opposite in sign. The physical torques are, however, applied in the same direction. From the figure, it is clear that, although the shuttle has rotated the prescribed amount, there is a small amount of residual torsional energy in the structure. This energy is due primarily to the deformation of the antenna. It is expected that additional penalties on structural deformation placed at various points on the antenna will significantly reduce this residual energy.

5. CONCLUSIONS

The open loop optimal control algorithm has been demonstrated for several structural models. The generality of the approach has been exploited in applying the algorithm to a complex structure. Furthermore, the ability of this approach to handle constraints and derivative penalties has been demonstrated. One major issue concerning this open loop method is modeling error. Because the approach presented is open loop, this formulation makes no guarantees on the performance of the actual structure, for which the mathematical abstraction is only an approximation. The necessary sensitivity analysis and closed loop formulations are topics of current research. It may also be possible to incorporate an adaptive identification algorithm to adjust the model in such a way as to minimize modeling error.

If the optimal control problem has an infinite time horizon, it is possible to use a different set of basis functions to converge on a solution. Candidate bases include Legendre and Laguerre functions, which are linear combinations of exponentials and other decaying functions.[14]

A method for incorporating distributed penalties into the optimal control algorithm is one topic of current research. Rather than penalizing certain points along a particular flexible element, an integral over the entire element, subject to some

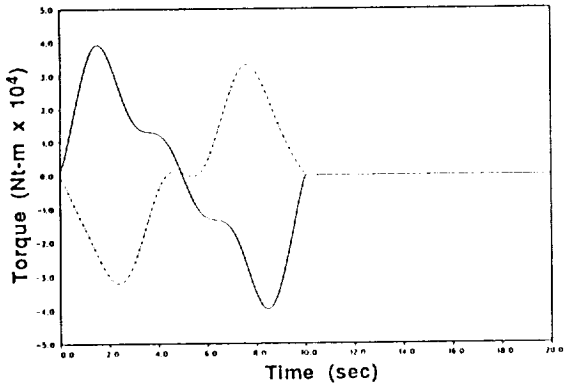

(a)

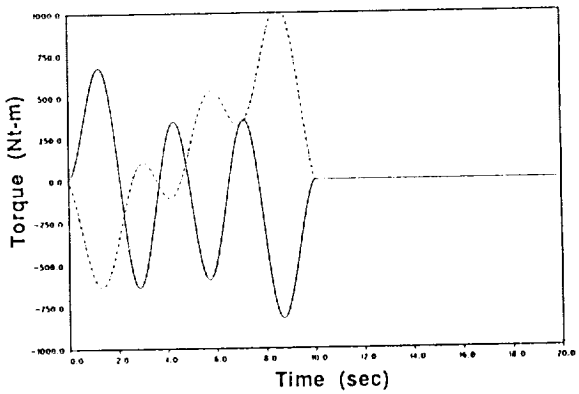

(b)

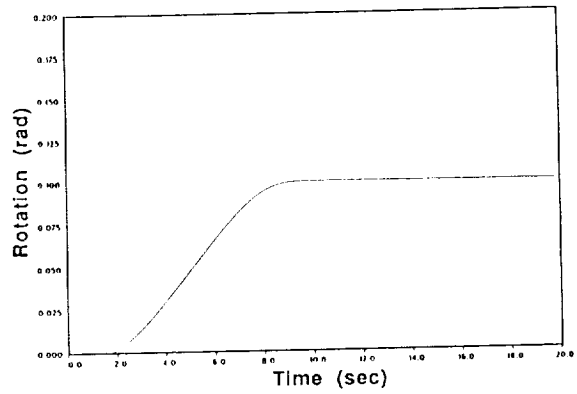

(c)

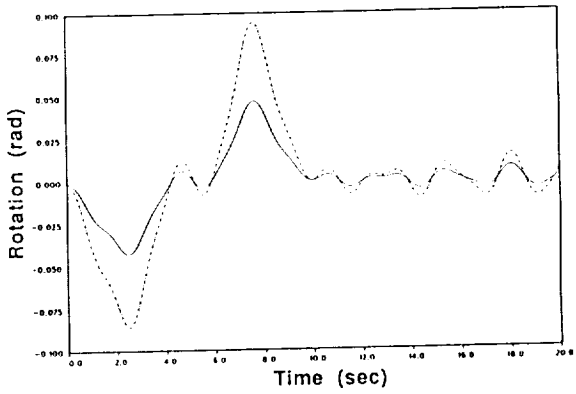

(d)

Fig. 12: Results of optimal SCOLE maneuver: (a) yaw torque applied to shuttle (solid line) and mast/antenna junction (dotted line), (b) roll torque (solid line) and pitch torque (dotted line) applied to shuttle, (c) yaw rotation of shuttle, (d) relative torsional deflection of mast at midpoint (solid line) and at mast/antenna junction (dotted line).

weighting function, becomes part of the cost functional. Such a capability would make it possible to develop controls that minimize the total (kinetic plus potential) energy within the structure in a continuous sense, rather than penalizing a large number of points within each flexible element.

Work is currently underway to extend the basic modeling approach to continuous plate and membrane elements. This capability will permit modeling and control formulations for the NASA space station class of large space structures.

ACKNOWLEDGEMENTS

The work has been sponsored by the AFOSR, under contract number 49620-89-C-0082.

REFERENCES

[1] Ketner, G.L., "Survey of Historical Incidences with Controls-Structures Interaction and Recommended Technology Improvements Needed to Put Hardware in Space," Internal Document, Pacific Northwest Laboratory, PNL-6846, UC-222, March, 1989.

[2] Tzafestas, S.G. and Nightingale, J.M., "Optimal Distributed Parameter Control Using Classical Variation Theory," *International Journal of Control*, Vol. 12, No. 4, 1970, pp. 593-608.

[3] Miller, D.W., Hall, S.R., and von Flotow, A.H., "Optimal Control of Power Flow at Structural Junctions," *Proceedings of the 1989 American Controls Conference*, Pittsburgh, PA., June, 1989, pp. 212-220.

[4] MacMartin, D. and Hall, S.R., "An H_∞ Power Flow Approach to Control of Uncertain Structures," Space Systems Laboratory Report No. 10-89, Massachusetts Institute of Technology, Cambridge, Ma.; Sept., 1989.

[5] Breakwell, J.A., "Optimal Control of Distributed Systems," Paper No. 80-1737, presented at the *AIAA Guidance and Control Conference*, Danvers, Ma., August, 1980.

[6] Skaar, S.B., "Closed Form Optimal Control Solutions for Continuous Linear Elastic Systems," *Journal of the Astronautical Sciences*, Vol. 32, No. 4, Oct.-Dec. 1984, pp. 447-461.

[7] Pichè, R.A., "Analysis of Structural Control Problems Using Frequency-Domain Continuum Methods," PhD Thesis, University of Waterloo, Waterloo, Ontario, 1986.

[8] Wittrick, W.H. and Williams, F.W., "A General Algorithm for Computing Natural Frequencies of Elastic Structures," *Quarterly Journal of Mechanics and Applied Mathematics*, Vol. 24, No. 3, 1971, pp. 263-284.

[9] Hildebrand, F.B., *Advanced Calculus for Applications*, Prentice-Hall, Inc., Englewood Cliffs, N.J., 1976.

[10] Wilcox, D.J., "Numerical Laplace Transform and Inversion," *Int'l J. of Electrical Engineering Education*, Vol. 15, 1978, pp. 246-265.

[11] Kulla, P.H., "Continuous Elements - Some Practical Examples," *Proc. ESTEC Workshop, Modal Representation of Flexible Structures by Continuum Methods*, ESTEC, Noordwijk, The Netherlands, June 15-16, 1989, pp. 171-192.

[12] Bailey, T.L., "Distributed Parameter Control of a Cantilever Beam Using a Distributed Parameter Actuator," SM Thesis, Massachusetts Institute of Technology, Cambridge, Ma., Sept. 1984.

[13] Taylor, L.W., and Balakrishnon, A.V., "A Mathematical Problem and a Spacecraft Control Laboratory Experiment (SCOLE) Used to Evaluate Control Laws for Flexible Spacecraft .... NASA/IEEE Design Challenge," NASA Technical Memorandum 89075, Nov. 17-18, 1986, pp. 386-412.

[14] Hall, S.R., Private communication, April, 1990.